Microsyst Technol (2012) 18:1549–1557
DOI 10.1007/s00542-012-1591-0

TECHNICAL PAPER

Contact between a thermal flying height control slider and a disk asperity

Wenping Song · Andrey Ovcharenko · Min Yang · Hao Zheng · Frank E. Talke

Received: 10 August 2011 / Accepted: 11 June 2012 / Published online: 22 June 2012

Abstract Contact between a thermal flying height control slider and an asperity on a disk is investigated using finite element analysis. The finite element model developed accounts for transient elastic–plastic deformation and heat generation due to frictional heating. Plastic deformation and temperature rise of the read/write element are determined as a function of flying height of the slider, location of the read/write element as well as material properties of typical disk asperities. The model shows good agreement with experimental data. Significant plastic deformation and temperature rise were observed in the shield and alumina regions of the slider. Hard and stiff disk asperities, such as alumina asperities, result in more damage to the slider than soft and compliant nickel-phosphorus ones.

1 Introduction

Due to the reduction of the head/media spacing, an increasing number of head and disk failures is likely to occur as a consequence of media defects. For example, localized heating of the magnetic media due to contacts between media defects and the slider can cause drop-out or distortion of the read signal, a highly undesirable situation. In general, contacts between media defects and a recording head are described as "thermal asperity" events (Stupp et al. 1999; Yuan and Liu 2000; Sharma et al. 2001a, b; Dorfman and Wolf 2001; Mathew and Tjhia 2005; Erden and Kurtas 2004). Many investigations have been performed in the past to understand and reduce the damaging effects of disk asperities on the head/disk interface. Yuan and Liu (2000) proposed a new head design to reduce the effect of localized temperature and stress fields on the read back transducer caused by head-disk impacts. Sharma et al. (2001a, b) observed that an air bearing surface (ABS) with a U-shaped slider rail and a central airflow channel reduces the damaging effects of disk asperities. In addition, several algorithms were proposed to detect and suppress read signal distortions and reduce bit errors due to the "thermal asperity" effect (Dorfman and Wolf 2001; Mathew and Tjhia 2005; Erden and Kurtas 2004). In the above references a number of methods were proposed to reduce the damaging effects of disk asperities, including modifications of the air bearing contour or changes in the read channel design. However, most of these ideas are difficult to implement. Moreover, none of the suggested methods has addressed the topic of localized frictional heating, although the latter is one of the main problems of asperity contacts. In particular, degradation of the read element can occur as a result of asperity contact since the effect of exchange bias in the reader structure vanishes when the temperature in the reader exceeds a critical temperature, the so-called "blocking temperature" (Kools 1996; Nogues and Schuller 1999; Pinarbasi et al. 2000). Whenever the blocking temperature is exceeded, the head cannot operate anymore, leading to failure of the disk drive.

Figure 1a shows a scanning electron microscope image of a typical disk asperity. The dashed line in Fig. 1a indicates the position at which the focused ion beam image shown in Fig. 1b

W. Song (✉)
School of Mechatronics Engineering,
Harbin Institute of Technology, Harbin, China
e-mail: wenping.song1985@gmail.com

W. Song · H. Zheng · F. E. Talke
Center for Magnetic Recording Research,
University of California, San Diego, CA, USA

A. Ovcharenko · M. Yang
Western Digital Corporation, San Jose, CA, USA

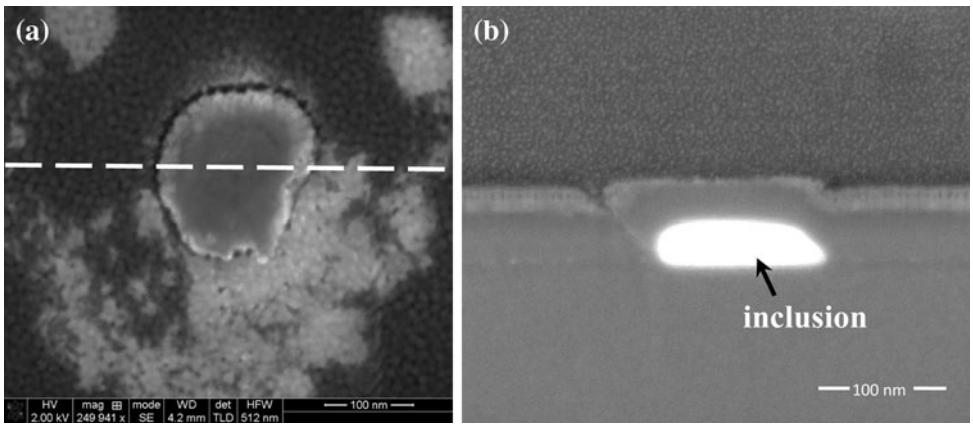

Fig. 1 Typical disk asperity: **a** SEM *top view* and **b** focused ion beam cross section

was obtained. From Fig. 1b we observe that a disk asperity is a physical defect or inclusion in the thin film coating of the disk. Inclusions of the type shown in Fig. 1b can consist of different materials (soft or hard) and can be observed in different locations. Typically, inclusions are introduced during the thin film deposition process. If additional layers are deposited on top of a typical inclusion, the geometry of the inclusion is enlarged to form a "shallow" defect on the surface of the disk. In addition to frictional heating, physical damage of the read/write head in the form of scratches or score lines (see Fig. 2) can be caused by contacts between an asperity and a magnetic recording slider. At present, no studies have been published on the tribology of asperity contact or the damage caused by transient contacts between disk asperities and magnetic recording sliders.

Thermal flying-height control (TFC) technology has been implemented in magnetic recording disk drives to reduce the flying height (FH) of the read/write element (Kurita et al. 2005; Zheng et al. 2009; Li et al. 2010). At present, the spacing between the read/write element and the disk is on the order of 1–2 nm, making contacts between asperities and the slider increasingly more likely. The goal of this study is to investigate the physical damage and temperature rise of the read/write element during contact between a TFC slider and a disk asperity. In particular, we will study the effect of flying height of the slider, the location of the read/write element on the slider and the effect of material properties of typical disk asperities.

2 Modeling

2.1 Theoretical model

Figure 3 shows the schematic of contact between a thermal protrusion on a TFC slider and an asperity on a disk. As can be seen from Fig. 3, the thermal protrusion on the slider is represented by a sphere with radius R_{TP}. The radius of the sphere is a function of the power applied to the heater of the

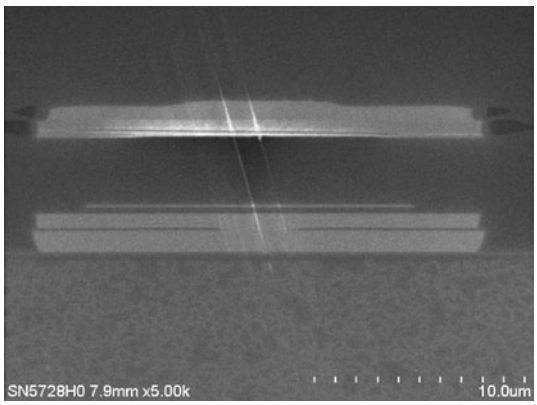

Fig. 2 SEM image of air bearing surface showing scoring of sensor region caused by a disk asperity

TFC slider. The asperity is modeled by a cylinder with a spherical cap of radius R on its top. Contact occurs between the asperity on the disk and the thermal protrusion of the slider if the height of the asperity is larger than the flying height of the slider. The flying height is defined as the spacing between the lowest point on the thermal protrusion of the slider and the surface of the disk (see Fig. 3). The geometry of the thermal protrusion and the disk asperity used in this study is also shown in Fig. 3. The equivalent radius of the thermal protrusion is chosen to be 5 mm, corresponding to the value of a typical thermal deformation obtained from numerical simulations using a model described by Li et al. (2010). The height and the radius of the asperity are assumed to be 15 and 2 μm, respectively, to represent the geometry of a typical asperity found on the disk surface as shown in Fig. 1. In our model, the carbon layer, the magnetic under layer, the intermediate layer and the magnetic recording layer of the disk are lumped into one representative layer in order to reduce the simulation time. Our approach allows modeling of individual media layers to represent more realistic media structures in future work.

In this study, the thermo-mechanical contact problem between a disk asperity and a thermal protrusion of a TFC

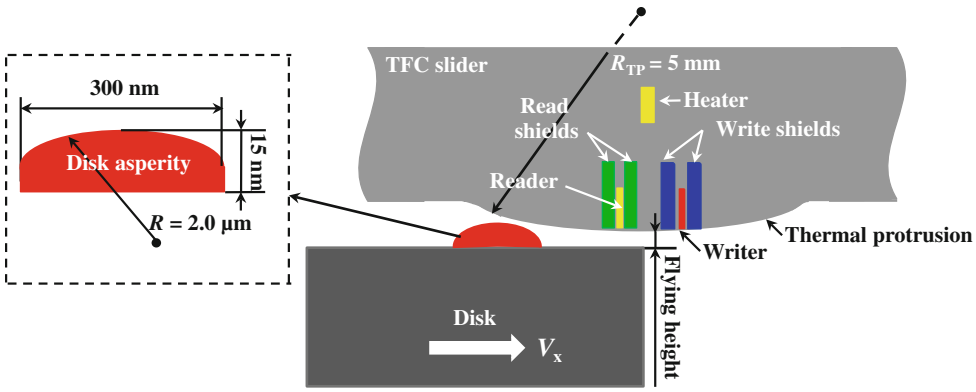

Fig. 3 Schematic of contact between thermal protrusion on TFC slider and asperity on disk

slider is simulated using LS-DYNA, a commercially available finite element solver (Hallquist 2006). The momentum equation and the thermal equilibrium equations are solved using explicit time integration and a backward integration scheme, respectively, as explained by Hallquist (2006). The thermal energy dissipated during a contact is assumed to be equal to the frictional energy generated. Thermal radiation and convection are not considered in our model. The surface temperature of the thermal protrusion of the slider and the disk asperity is assumed to be the same at opposing nodes in the contact interface to fulfill the Block postulate (Block 1937).

2.2 Material model

In our study, a thermo-elastic–plastic material model as described by Hallquist (2006) was used in the same way as used by Ovcharenko et al. (2010, 2011). This model allows the use of temperature dependent material properties. Stress is calculated based on elastic and thermal strain. When treating plasticity the stress is updated elastically and checked whether it exceeds the isotropic yield function

$$\phi = \frac{1}{2} S_{ij} S_{ij} - \frac{\sigma_Y(T)^2}{3} \tag{1}$$

where S_{ij} is the deviatoric stress tensor and σ_Y is the yield strength in uniaxial tension. If the stress exceeds the elastic limit, the stress deviators are scaled back by a factor f_s, i.e., $S_{ij}^{n+1} = f_s S_{ij}$, where the factor f_s is defined as:

$$f_s = \frac{\sigma_Y}{\sqrt{\frac{3}{2} S_{ij}^* S_{ij}^*}} \tag{2}$$

The plastic strain is updated by the increment

$$\Delta \varepsilon_{eff}^p = \frac{(1 - f_s)\sqrt{\frac{3}{2} S_{ij}^* S_{ij}^*}}{G + 3E_p} \tag{3}$$

where G is the shear modulus and E_p is the plastic hardening modulus, assumed to be equal to 2 % of the Young's modulus.

The material properties of the read–write shields, the slider and the disk correspond to the material properties of NiFe, alumina (Al_2O_3) and NiP, respectively. Two types of asperities were studied, NiP and Al_2O_3. Table 1 shows a summary of the material properties used.

2.3 Finite element model

Figure 4 shows the finite element model of the slider and the disk asperity developed using the commercially available software Hypermesh. Since the thickness of the read and write elements is much smaller than the thickness of the shields, we neglected the effect of the thickness of the read and write elements in comparison with the thickness of the shields. Current heads have multiple shields for read and write elements. In this study we modeled multiple shields by a representative shield with the combined thickness of the multiple shields. The combined thickness of the read shields was assumed to be 1,490 nm while the combined thickness of the write shields was 2,370 nm. The extent of the Al_2O_3 region between the read and write shields was assumed to be 2,730 nm. These dimensions correspond to typical dimensions of TFC sliders in current day hard disk drives.

The lateral dimension of the region denoted as Al_2O_3 #1 in Fig. 4 was selected as a function of the flying height of the slider and the initial contact location. For the numerical calculations, typical dimensions of the thermal protrusion

Table 1 Mechanical and thermal material properties

	NiP	Al_2O_3	NiFe
Young's modulus, E (GPa)	114	400	205
Yield strength, Y (GPa)	3.0	6.4	1.7
Density, ρ (kg/m^3)	8,000	3,890	8,440
Poisson ratio, v	0.31	0.23	0.22
Thermal expansion coefficient, (10^{-6} K^{-1})	13.3	5.5	12
Heat capacity, H (J kg^{-1} K^{-1})	440	780	440
Thermal conductivity, k (W m^{-1} K^{-1})	4.4	1.3	35

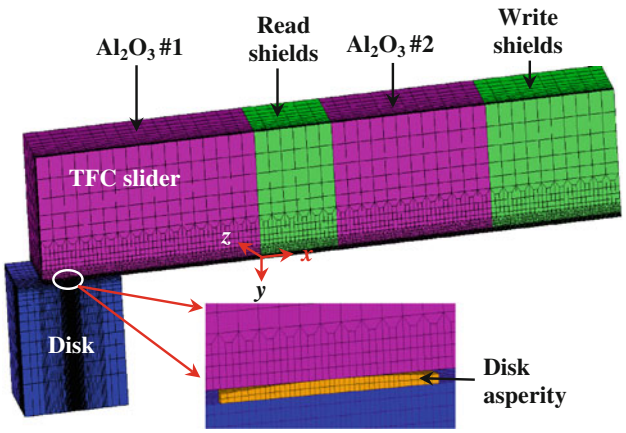

Fig. 4 Finite element model of contact between thermal protrusion on TFC slider and asperity on disk

of the slider in the y and z directions were chosen to be 2,000 and 1,500 nm, respectively. Dimensions of a typical disk asperity are given in Sect. 2.1. The entire model consists of approximately 180,000 eight-node hexahedral elements and 160,000 nodes depending on the flying height of the slider. The smallest element size within the contact zone is 6.7 nm × 6.7 nm × 8.0 nm in the x, y and z directions, respectively.

The asperity on the disk moves with a constant velocity of $V_x = 20$ m/s in the x-direction. The mass of the slider was assumed to be 0.5 mg. The coefficient of friction between slider and disk asperity was chosen to be $\mu = 0.2$.

Since the numerical problem is symmetrical with respect to the xy plane, we have considered only one half of the contact problem shown in Fig. 4. The following boundary conditions are imposed:

- The displacement is zero in the z direction for nodes lying in the xy plane due to symmetry.
- The displacement of nodes at the bottom of the disk is zero in the y and z direction, respectively.
- The nodes at the top of the slider are restrained from moving in the x and z direction, respectively.
- The initial temperature in the slider (Al_2O_3 #1) is assumed to be 315 K. The initial temperature in the read shield, write shield, and alumina area of the slider (Al_2O_3 #2) is assumed to be 335 K, respectively, while the initial temperature of the disk and the asperity is assumed to be 300 K. The elevated temperature of the slider with respect to the disk is related to the heater in the slider as described by Li et al. (2010).

The thermo-mechanical finite element model was verified similar to the procedure used by Ovcharenko et al. (2010, 2011). At first, proper convergence of the numerical solution was tested by increasing the number of elements until further mesh refinement resulted in a change of less than 1.5 % for the maximum plastic strain, the maximum residual deformation and the maximum contact force. After that, the mechanical response of the model was verified by assigning the same material properties for the whole TFC slider and comparing the results with the analytical impact solution of Hertz (Johnson 1985). The disk tangential velocity was set to zero and a vertical initial velocity in the elastic regime of deformation was given to the TFC slider. The error for the maximum value of contact load, contact area and contact time was found to be <3.3 %. Thereafter, the thermal response was validated by comparing the steady-state maximum surface temperature rise with the approximate analytical solution of Tian and Kennedy (1994). To validate the numerical results, a constant normal load and tangential velocity were applied to the TFC slider keeping the disk with the asperity fixed at the bottom. The difference between the analytical and numerical results was found to be <3 %. To obtain a converged solution for a single case, a computation time of approximately 2 days was needed using a HP workstation with four CPUs and 8 GB RAM running at 2.8 GHz.

3 Results and discussion

Figure 5 shows a typical result for (a) contact force and (b) temperature rise on the top of an Al_2O_3 disk asperity as a function of contact time assuming $V_x = 20$ m/s, $FH = 2$ nm and $\mu = 0.2$. As shown in Fig. 5a and b, both the contact force and the temperature rise can be divided into four regions denoted as I, II, III and IV. During transient contact the disk asperity is first in contact with the region denoted Al_2O_3 #1, then with the read shields, thereafter with the region Al_2O_3 #2, and, finally, with the write shields (see Fig. 4). We can observe from Fig. 5a that the maximum contact force in regions I is larger than the maximum contact force in region II, and that the maximum contact force in region III is larger than the maximum contact force in region IV. This is due to the fact that the Young's modulus of Al_2O_3 in regions I and III is larger than that of the read and write shields in regions II and IV. A large contact force in regions I and III leads to increased frictional heating and results in a large temperature rise (see Fig. 5b). Another important reason for the large temperature rise in regions I and III is that the thermal conductivity of Al_2O_3 is lower than that of the read and write shields (see Table 1). We observe from Fig. 5 that the total contact time between a disk asperity and the thermal protrusion of the slider is very short and typically a fraction of a microsecond. In the tribology literature the temperature rise occurring during short contacts is known as "flash temperature" (Suzuki and Kennedy 1989; Yu et al. 2008; Ovcharenko et al. 2011). One of the main objectives of this

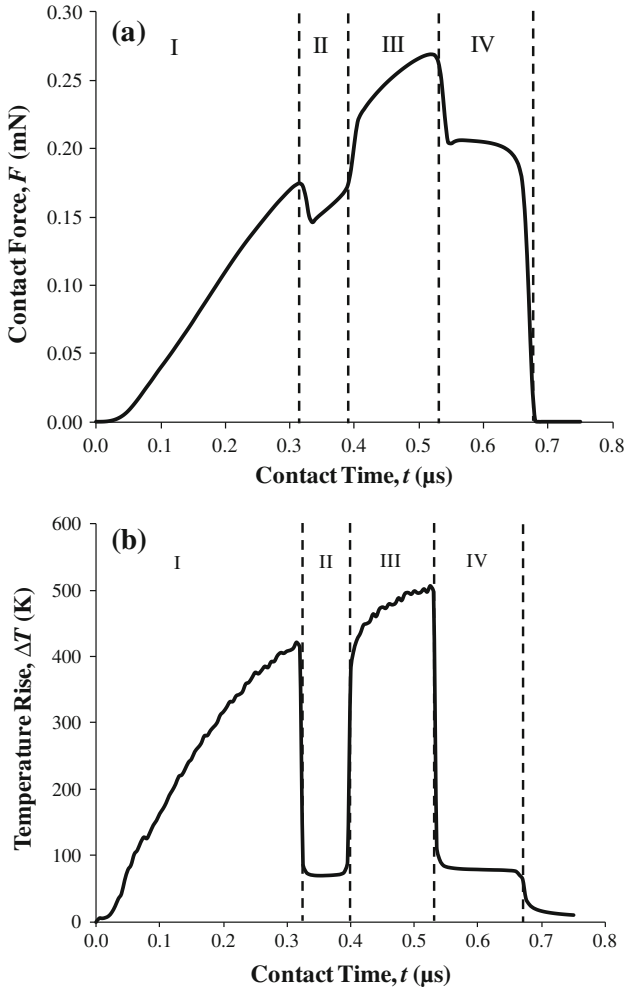

Fig. 5 Typical result for **a** contact force and **b** temperature rise on the top of an Al_2O_3 disk asperity as a function of contact time assuming $V_x = 20$ m/s, $FH = 2$ nm, $\mu = 0.2$

paper is to evaluate the maximum temperature rise of the "reader" and compare this temperature to the reader blocking temperature (Kools 1996; Nogues and Schuller 1999; Pinarbasi et al. 2000), i.e., the temperature above which degradation of the reader is likely.

In this investigation, two different modes are considered for the operation of a TFC slider, the "write mode" and the "read mode". These modes relate to the position of the read and write elements relative to the thermal protrusion on the slider. A schematic model of the write and read modes, respectively, is shown in Fig. 6. As can be seen from Fig. 6a, the write element is positioned on the thermal protrusion in such a way that the write element is the "lowest" point on the thermal protrusion of the slider. This mode is called the write mode. On the other hand, if the lowest point on the thermal protrusion of the slider is at the read element (see Fig. 6b), the so-called read mode is presented. Thermal flying height control sliders can operate in either the write mode or the read mode, depending on the

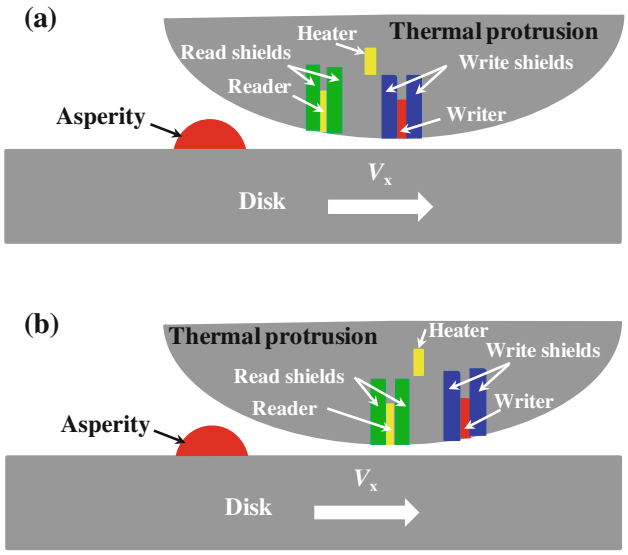

Fig. 6 Schematic of **a** the write mode and **b** the read mode during operation of a TFC slider

design of the air bearing and the heater element. If slider designs are used with two independent heaters, as proposed by Zheng et al. (2009), the same head can be used to operate in either the read mode or the write mode, depending on the power input for each of the two heaters.

Figure 7 shows the distribution of the plastic strain at the bottom surface of the thermal protrusion of a typical TFC slider during (a) the write mode and (b) the read mode for different values of the flying height of the slider. We observe from Fig. 7 that the size of the plastic region and the magnitude of the plastic strain in the region of the read and write shields increases with a decrease in the flying height of the slider. However, plastic deformation is not observed in the alumina (Al_2O_3 #2) due to the high yield strength of this material. In addition, we observe from Fig. 7a that the plastic strain in the write shields is larger than that in the read shields during the write mode. This result is related to the design of the TFC slider under investigation, i.e., the write element is closer to the disk than the read element during the write mode. We also observe that the plastic strain in the read shields is larger than that in the write shields during the read mode (see Fig. 7b). Again, this result is related to the position of the read element during the read mode, i.e., the read element in this slider is closer to the disk than the write element during the read mode.

Figure 8 shows an atomic force microscopy image of "scoring" marked on the thermal protrusion region of a typical TFC slider, consisting of deep scratches in both the read and the write shields. The scratches are the result of contact of the slider with an alumina asperity. On the other hand, scratches in the Al_2O_3 region are absent.

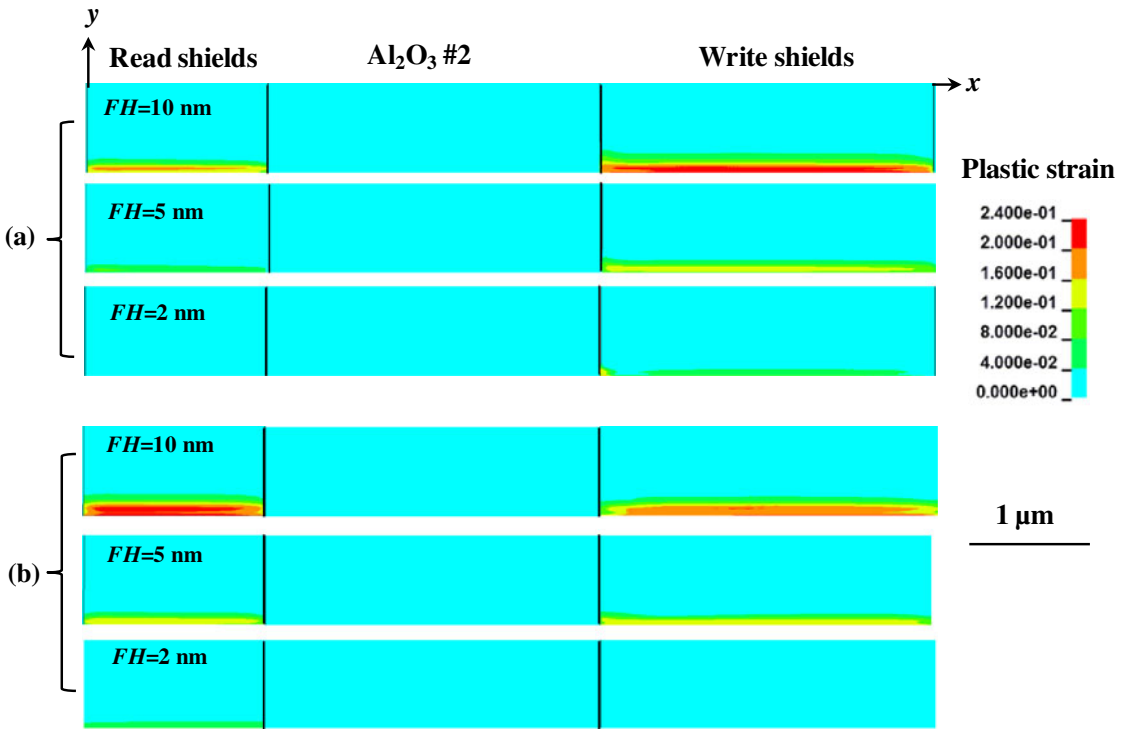

Fig. 7 Distribution of plastic strain at the bottom surface of a thermal protrusion of a TFC slider during **a** write mode and **b** read mode for different values of flying height of the slider

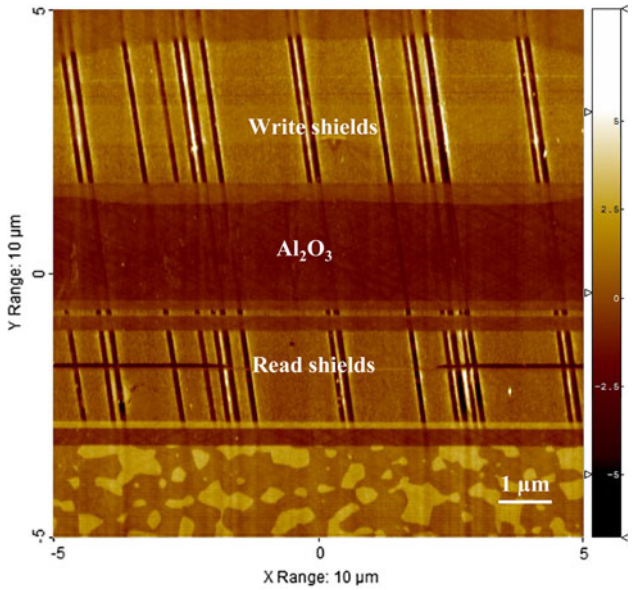

Fig. 8 Atomic force microscope image of "scoring" in a slider due to contact with a disk asperity

Figure 9a shows the profile of typical scratches in the soft write shields as a function of flying height obtained from numerical simulations while Fig. 9b shows a typical scratch from an experimental measurement after contact between a TFC slider and a disk asperity. Comparing the results of the scratch width and depth, we observe that the numerical calculations are in good qualitative and quantitative agreement with the experiential results. In this study, the scratch depth D and the scratch width W were defined as the maximum values of plastic deformation due to a single transient contact. The scratch depth and scratch width for a flying height of 2 nm are shown in Fig. 9a.

Figure 10a and b show the scratch depth D and the scratch width W in the read and write shields, respectively, as a function of the flying height of the slider during the write mode. We observe that the values of the scratch depth and scratch width in the write shields are larger than those in the read shields. This is in agreement with the plastic strain distribution shown in Fig. 7a.

Figure 11a and b show the scratch depth D and the scratch width W in the read and write shields, respectively, as a function of the flying height of the slider during the read mode. Contrary to the results shown in Fig. 10, the values of the scratch depth and scratch width in the read shields are now larger than those in the write shields. This is due to the position of the read shields on the thermal protrusion of the slider, i.e., the read shields are closest to the disk surface during the read mode. This result is in good qualitative agreement with the plastic strain results shown in Fig. 7b.

Figure 12 presents the maximum temperature rise in the TFC slider as a function of the distance from the read shields for several values of the flying height of the slider.

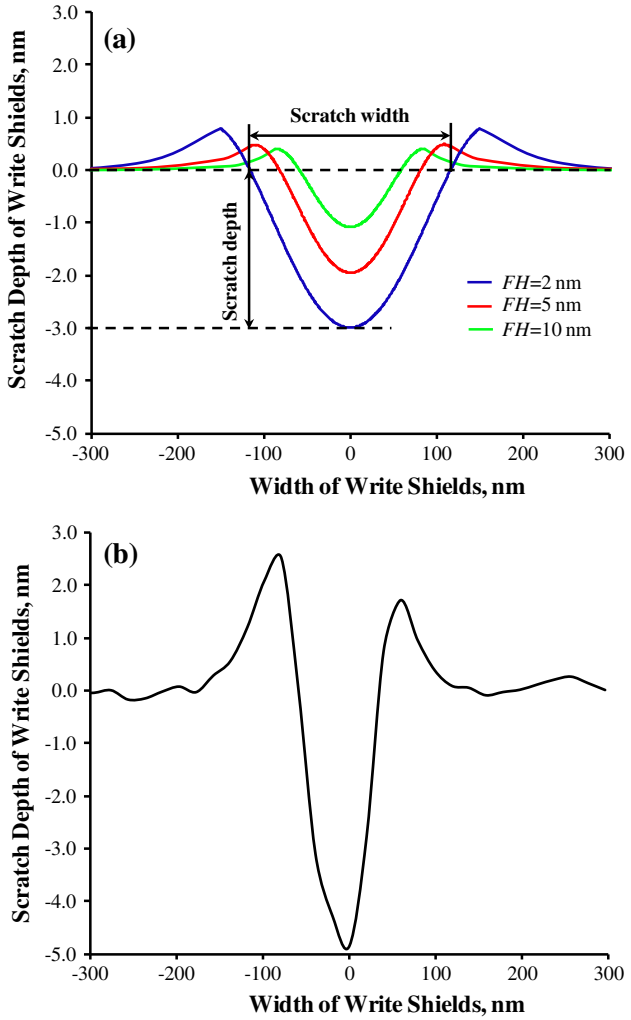

Fig. 9 **a** Typical scratches on write shields obtained from simulation; **b** experimental measurement of typical scratch profile at maximum scratch depth

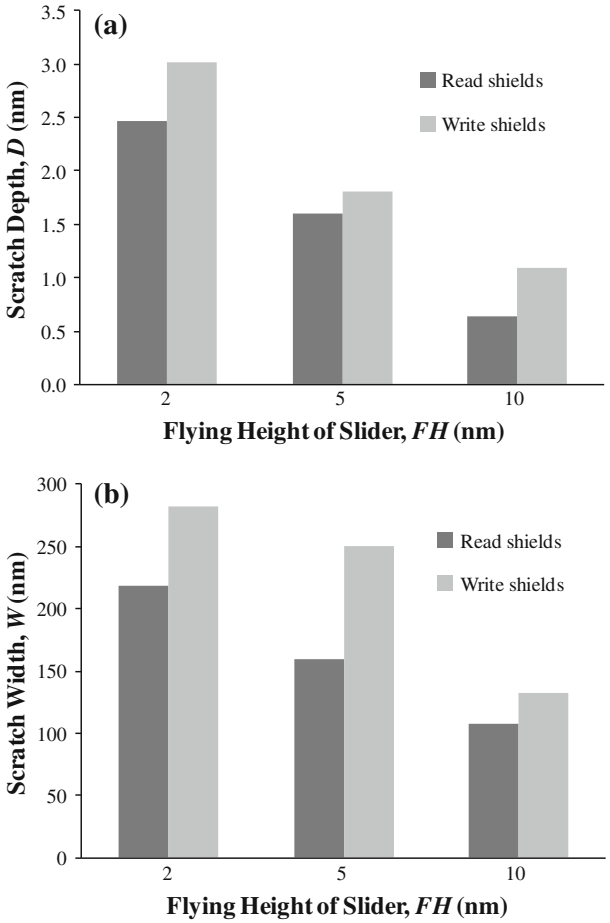

Fig. 10 Scratch dimensions in read and write shields: **a** scratch depth and **b** scratch width as a function of flying height of a TFC slider during the write mode

The maximum temperature rise for the write mode and the read mode is marked by solid and dashed lines, respectively. We observe that the maximum temperature rise increases with a decrease in the flying height of the slider. For the same value of flying height, the maximum temperature rise in the read shields is higher than in the write shields during the read mode. On the other hand, the maximum temperature rise in the write shields is higher than that in the read shields during the write mode. In addition, we observe that the maximum temperature rise in the region denoted as Al_2O_3 #2 is much higher than that in the read and write shields. For example, at a flying height of 2 nm, the maximum temperature in the region Al_2O_3 #2 increases by 450 K but only by about 45 K in the read shields. This is due to the fact that the thermal conductivity of NiFe (i.e., the material of the read and write shields) is about 30 times larger than that of Al_2O_3 (see Table 1). It is important to note that the blocking temperature of a reader is around 470 K (Kools 1996; Nogues and Schuller 1999; Pinarbasi et al. 2000). From our simulation results we observe that the maximum temperature of the read shields reaches 380 K. This temperature is well below the blocking temperature of the reader. However, our preliminary results suggest that higher tangential disk velocities and an increase in the coefficient of friction could potentially increase the maximum temperature of the reader to exceed the blocking temperature.

Figure 13 gives a comparison of the scratch depth in Fig. 13a and the scratch width in Fig. 13b in the write shields as a function of the flying height of the slider during the write mode for NiP and Al_2O_3 disk asperities. We observe that the values of the scratch depth and the scratch width for the Al_2O_3 disk asperity are larger than those for the NiP disk asperity. This is due to the fact that the values of the Young's modulus and the yield strength of Al_2O_3 are larger than those of NiP (see Table 1) leading to higher contact force and larger residual plastic deformation.

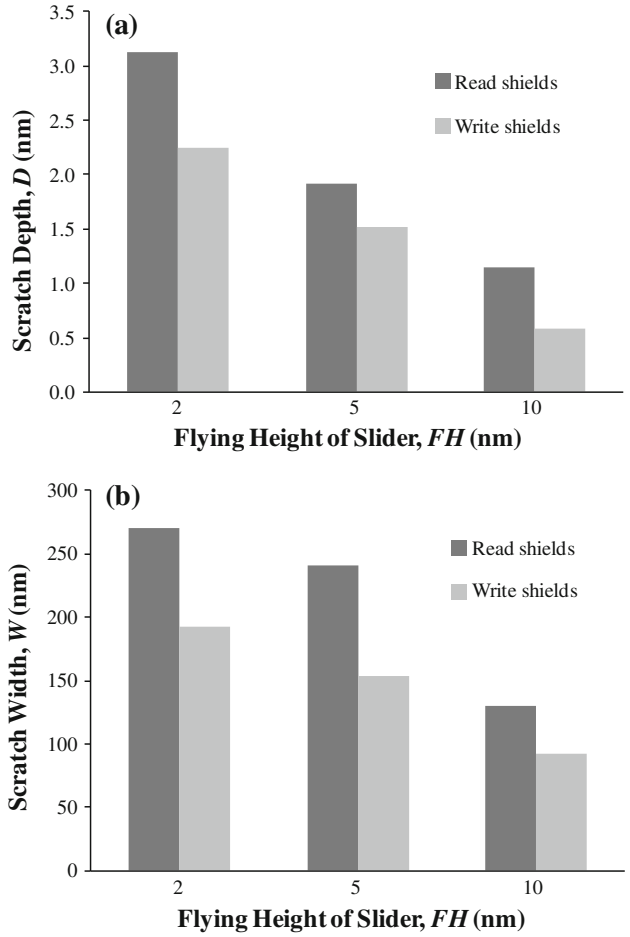

Fig. 11 Scratch dimensions in read and write shields: **a** scratch depth and **b** scratch width as a function of flying height of the slider during read mode

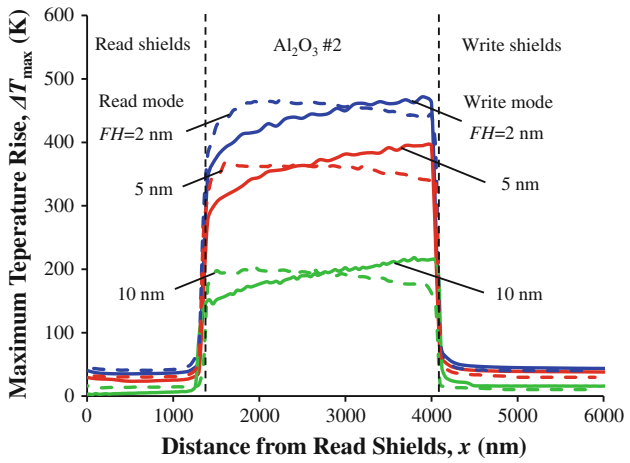

Fig. 12 Maximum temperature rise in TFC slider for different values of flying height of the slider for the case of an Al_2O_3 disk asperity

In Fig. 14, the maximum temperature rise in a typical TFC slider is shown as a function of the distance from the read shields for an alumina and a nickel-phosphorus disk

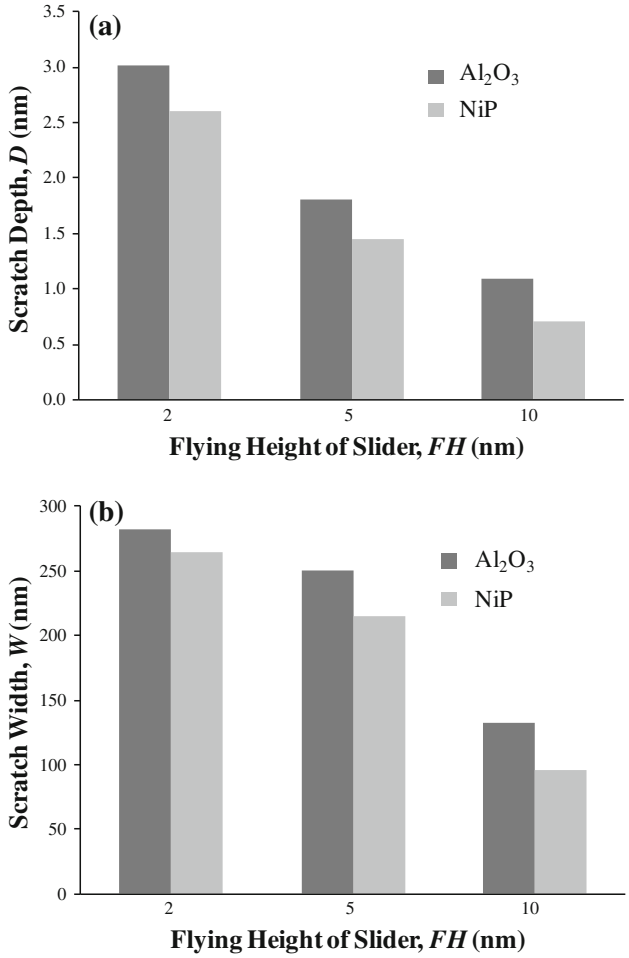

Fig. 13 Scratch dimensions in write shields: **a** scratch depth and **b** scratch width as a function of flying height of the slider during write mode

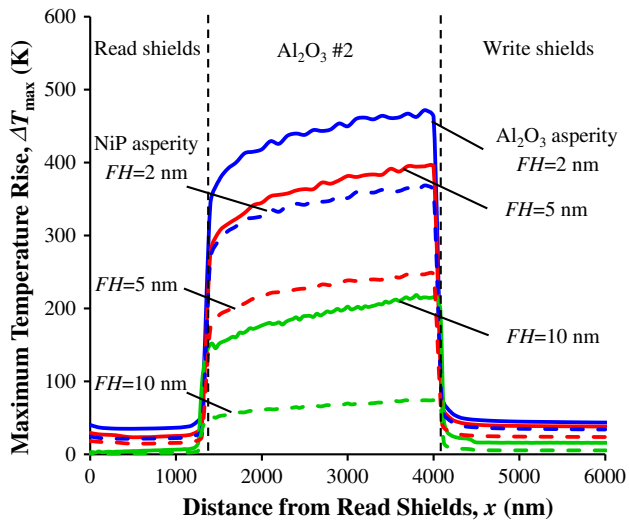

Fig. 14 Maximum temperature rise in a TFC slider for different values of flying height of the slider and different material properties of disk asperity. The results for Al_2O_3 and NiP disk asperities were denoted by solid and dashed lines, respectively

asperity, denoted by solid and dashed lines, respectively. The maximum temperature rise was calculated for several values of the flying height. We observe that for the same value of flying height the maximum temperature rise is higher for a disk asperity of Al_2O_3, than for one of NiP. Again, this result is related to contact force and frictional heating of each disk asperity type. In addition, the thermal conductivity of NiP is larger than that of Al_2O_3, and therefore dissipates frictional heating more efficiently than the alumina disk asperity.

4 Conclusions

A thermo-elastic–plastic transient contact model was used to investigate the mechanical and thermal responses of the read/write elements of a TFC slider during contacts with disk asperities of alumina and nickel-phosphorus. The following conclusions can be made:

1. Contact between a disk asperity and a TFC slider can cause plastic deformation and a large temperature rise.
2. Both the scratch depth and the scratch width increase with a decrease in the flying height of a TFC slider. The scratch dimensions are strong functions of the location of the read and write elements with respect to the "thermal protrusion" of the slider.
3. Scratches on the slider are deeper and wider for disk asperities of rigid and hard Al_2O_3 compared to asperities of soft and compliant NiP.
4. For the cases studies, the maximum temperature rise in the read and write shields was found to be about 45 K while the temperature rise in the Al_2O_3 region was found to be as large as 450 K.

Acknowledgments We would like to thank Dr. Raj Thangaraj, Dr. John Ji and Dr. Leo Volpe from Western Digital Corporation for helpful discussions with this paper. Wenping Song thanks the China Scholarship Council (CSC) and Prof. Guangyu Zhang from Harbin Institute of Technology, for supporting his Ph.D. studies at UCSD.

References

Block H (1937) Theoretical study of temperature rise at surfaces of actual contact under oiliness lubricating conditions. Proc Inst Mech Eng Gen Discuss Lubr 2:222–235

Dorfman V, Wolf JK (2001) A method for reducing the effects of thermal asperities. IEEE Trans Magn 19(4):662–667

Erden MF, Kurtas EM (2004) Thermal asperity detection and cancellation in perpendicular magnetic recording systems. IEEE Trans Magn 40(3):1732–1737

Hallquist JO (2006) LS-DYNA theoretical manual. Livermore Software Technology Corporation, Livermore

Johnson KL (1985) Contact mechanics. Cambridge University Press, Cambridge

Kools JCS (1996) Exchange-biased spin-valves for magnetic storage. IEEE Trans Magn 32(4):3165–3184

Kurita M, Xu J, Tokuyama M, Nakamoto K, Saegusa S, Maruyama Y (2005) Flying-height reduction of magnetic-head slider due to thermal protrusion. IEEE Trans Magn 41(10):3007–3009

Li H, Zheng H, Fritzsche J, Amemoya K, Talke FE (2010) Simulation of flying height and response time of thermal flying height control sliders with thermal insulators. IEEE Trans Magn 46(6):1292–1294

Mathew G, Tjhia I (2005) Thermal asperity suppression in perpendicular recording channels. IEEE Trans Magn 41(10):2878–2880

Nogues J, Schuller IK (1999) Exchange bias. J Magn and Magn Mat 192:203–232

Ovcharenko A, Yang M, Chun K, Talke FE (2010) Simulation of magnetic erasure due to transient slider-disk contacts. IEEE Trans Magn 46(3):770–777

Ovcharenko A, Yang M, Chun K, Talke FE (2011) Transient thermomechanical contact of an impacting sphere on a moving flat. ASME J Tribol 133:031404

Pinarbasi M, Metin S, Gill H, Parker M, Gurney B, Carey M, Tsang C (2000) Antiparallel pinned NiO spin valve sensor for GMR head application. J Appl Phys 87(9):5714–5719

Sharma V, Kim SH, Choa SH (2001a) Head and media design considerations for reducing thermal asperity. Tribol Int 34(5):307–314

Sharma V, Kim SH, Choa SH (2001b) The effects of slider design on thermal asperity rejection capability. J Mech Sci Technol 15(3): 281–290

Stupp SE, Baldwinson MA, Mcewen P (1999) Thermal asperity trends. IEEE Trans Magn 35(2):752–757

Suzuki S, Kennedy FE (1989) Measurement of flash temperature and contact between slider and magnetic recording disk. IEEE Trans Magn 25(5):3728–3730

Tian X, Kennedy FE (1994) Maximum and average flash temperatures in sliding contacts. ASME J Tribol 116(1):167–174

Yu N, Polycarpou AA, Hanchi JV (2008) Elastic contact mechanics-based contact and flash temperature analysis of impact-induced head disk interface damage. Microsyst Technol 14(2):215–227

Yuan Z, Liu B (2000) Anti-thermal asperity head: design and performance analysis. J Magn Magn Mater 209(1–3):166–168

Zheng H, Li H, Talke FE (2009) Numerical simulation of a thermal flying height control slider with dual heater and insulator elements. IEEE Trans Magn 45(10):3628–3631